

## Shape Memory Wires As Artificial Muscles: An Experimental Approach

Amit Swamy

Emirates College of Technology, Abudhabi, UAE.

**Article History:** Received: 11 January 2021; Revised: 27 February 2021; Accepted: 27 March 2021; Published online: 10 May 2021

**Abstract** – The paper discusses various simulation and modelling techniques adopted by researchers, that are discussed individually and then collectively with regard to their relevance to the current work. The intervertebral disc muscles and vertebral bones are critical components of the spine. So, a simplified model of an intervertebral disc is developed and subjected to compressive flexion and torsional loading. The effects of different artificial muscles are investigated and the results are compared with the experimental data of mammalian muscles

The long-term goal is to develop an artificial laboratory spine with active muscles that could be used to test spinal devices and instrumentation.

**Keywords** – Lower back muscles, artificial muscles, shape memory alloy, martensitic, austenite.

### I. INTRODUCTION

The lumbar spine contains five moderately large vertebrae, which sit above each other as shown in figure 1.1.

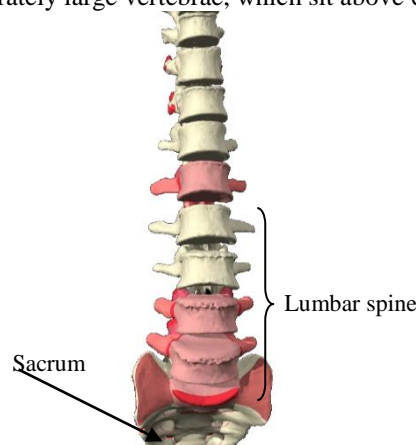


**Figure 1.1** Structure of lumbar spine with vertebral bodies. (Modified from Noordeen et al, 2001)

The transverse and spinous processes acts as attachments for muscles and ligaments in the lumbar spine and also encase and protect the lower spinal cord and lumbar nerve roots. For simplification purposes, the flexor and extensor muscles of the lumbar spine can be classified depending on their functional abilities as discussed in Gray et al, 1987; where the classification is based on the grades of muscles that are dependent on their positions and functions. The extensor and flexor muscles are attached directly or indirectly to the processes of the vertebrae, and can be classified into different grades of muscles, which fill the vertical gap posterior to the transverse processes and lateral to the spinous processes.

According to Gray et al, 1987; the Grade 1 extensor segmental muscles, such as supra-spinalis and interspinales, transverses and inter-transverses, are short muscles that act as antagonistic pairs for each intervertebral disc rotations as shown in figure 1.2 and 1.3. The interspinales lie on the spinous processes and connect to the spinous process of the adjacent lumbar vertebrae. The transverses and intertransverses are connected to the transverse processes that act as fine tune or antagonistic pairs for imbalanced movements.

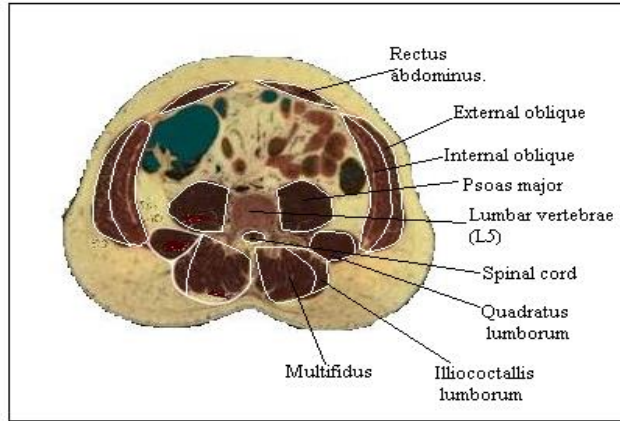


**Figure 1.2 Cadaveric cross-sections of lumbar vertebrae (L5).**(Modified from Noordeen et al, 2001)

The Grade 2 extensor multi-segmental muscles have multiple attachments depending on their physical positions and are the multifidus, ilicostalis, longissimus. Van et al (1997) describe the multifidus muscle as having a number of bundles of muscle fibres (fasciculi), which are attached to the spinous processes of each vertebra, and form one of the largest of the back muscles, as shown in figure 1.3 The longissimus runs from L1 to the Sacrum with some fascicles connected to the transverse processes of vertebral bodies. The Grade 3 extensor muscles lie lateral to the multifidus and are observed as a flat sheet of collagen fibres and muscles are responsible for the major movements of the vertebral bodies, of lifting and lowering.

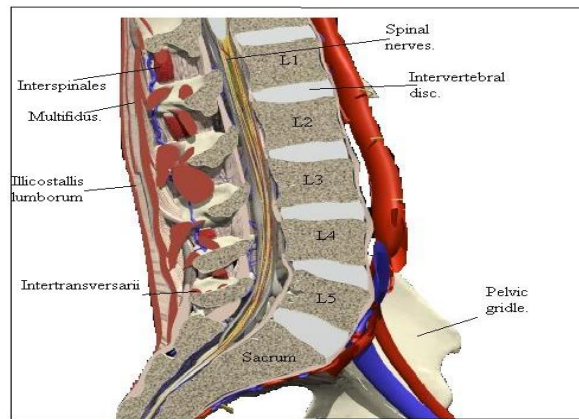
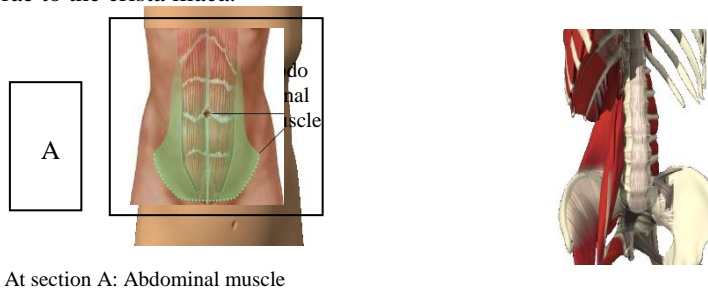


**Figure 1.3 Extensor muscles of lumbar region in sagittal plane.** (Modified from Noordeen et al, 2001)

The flexor muscles attach to the anterior location of the spine generally in the abdominal parts, as shown in figure 1.4. The Grade 1 flexor muscles are called poly-functional muscles due to the multiple functions that they perform, and include the quadratus lumborum, psoasmajor, internal and external oblique.

The psoasmajor is divided into different fascicles, with each fascia originating from the vertebral bodies (Bogduk et al, 1997). They start from thoracic 12 (T12) and are attached to the transverse and spinous processes of the lumbar vertebrae. The psoas major is attached to the trochanter with an intersection point on the pelvis. The quadratus lumborum, contributes towards lateral flexion, as well as providing support during respiration. The quadratus lumborum originates from the 12<sup>th</sup> rib and connects the transverse processes of upper four lumbar vertebrae to the crista iliaca.



At section A: Abdominal muscle

**Figure 1.4 Anterior flexor muscles.**  
(Modified from Noordeen et al, 2001 and 1997)

The Grade 1 flexor muscles are shown in figure 1.4; muscles which are connected to the abdomen (i.e. rectus abdominis), quadratus lumborum and the abdominal pressure. This abdominal musculature and the intra-abdominal pressure have a combined effect on flexure of the spine, where the flexor muscles support the extensor muscles by parallel or antagonistic activation during movements.

There are many sources of reference which describe the anatomy and function of the spine in detail; for example: Bogduk et al (1997), Dean and Pegington (2002), Gray et al (1987), Molly and Blume (2001), Schmorl and Junghans (1971), Van et al (1997).

## II. MUSCLE ARCHITECTURE

The lumbar spine is a complicated structure with very complex musculature and control. The entire human lumbar spine with all geometrical complexity physiologically performs all movements of the body. These movements are generated from the biomechanical movements of the different vertebral bodies connected to the lumbar spine that as explained causes different behaviour of the intervertebral discs. A very complex architecture of muscles and ligaments surrounds the vertebral bodies. The physiological movements are caused by different muscle activation connected to various processes of the vertebral bodies. The muscles considered in the lumbar spine model of Shirazi-Adl et al (2002) had extensor and flexor muscles modelled with different processes of lumbar vertebral body as shown in figure 1.5.

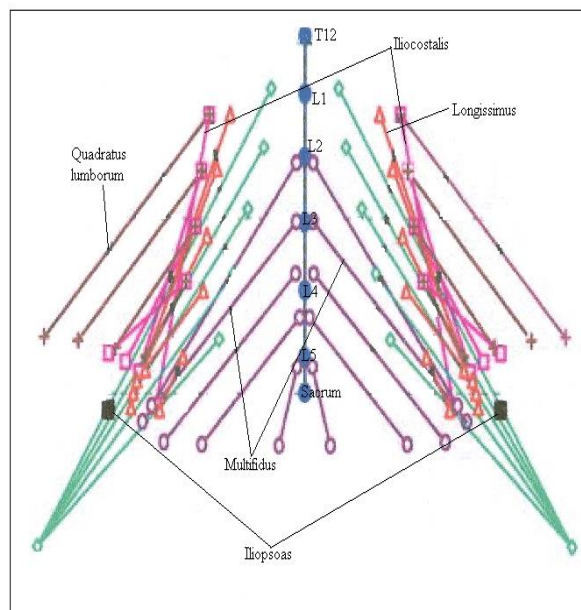


**Figure 1.5 Artificial muscle attachments.**  
(Modified from Shirazi-Adl et al, 2002)

The use of cadaveric tissue to examine the biomechanical characteristics of individual components or sections of the spine is fraught with difficulties. Firstly, the method of storage will affect the results of the tests and the general condition of the sample. Secondly, it seems highly unlikely that the properties of dead tissue will be representative of living tissue, hence range of motion data, should be treated with caution. This may also explain why there is often variability between different researcher's results. Finally, the effect of diseases will affect the properties hence the source of material also needs to be considered carefully.

## III. ARTIFICIAL MUSCLES

The muscles in the human body convert chemical energy to mechanical energy. The live muscle cells are capable of adopting a variety of shapes and can carry out coordinated and directed movements that depend on the bone geometry and activities required. The muscles in the human body are a bunch of fibres, which contract and expand depending upon the control.

In this section, ideas for artificial muscle are discussed, with the aim of creating a similar force-length relationship to represent the actual musculature. Also the different control methodologies are introduced.

The ligaments and muscles for the physical model essentially need to be elastic bands and force actuators respectively, depending upon the actuation process and functions. Various options are possible including magnetostrictive materials, electrostrictive materials, shape memory materials and simple mechanical mechanisms. Each of these options is now reviewed.

### Magnetostrictive materials.

Magnetostriction is a property of a magnetostrictive material which can undergo a change in physical dimension due to a change in the state of magnetization. The history of magnetostriction begins in early 1840, when James Prescott Joule identified the change in length of an iron sample as its magnetization changed, which is now known as the Joule effect (Wayman et al 1983).

The most common form of magnetostrictive material available in commercial quantities, is Terfenol-D which contains two rare earth elements, terbium (Tb) and dysprosium (Dy). The magnetostriction can be modified in two ways, firstly by raising the level of Tb so enhancing the magneto-elastic performances and secondly by slightly reducing the amount of iron content (Fe) which increases the magnetization. A recent development with composition  $Tb_{0.37}Dy_{0.7}Fe_{1.95}$  has a slight excess of rare earth material at grain boundaries, so that the material is less brittle than normal. The material has Young's modulus between 25-35 GPa (Zhou and Lau, 2001).

The operation of magnetostrictive materials like Terfenol-D can be understood using a simple ellipse model as shown in figure 1.6. The material may be thought of as an ellipse where the magnetization runs along the major axis. Applying a field to the ellipse has the result of rotating the magnetization in the direction of the field and subsequently producing a change in shape.

The disadvantages of magnetostrictive materials as discussed by Heremans (1983) are that they are expensive with a large magnetic field that makes the control complicated. Also, the relatively small displacements (albeit produced with a large resultant force) require large amplifications.

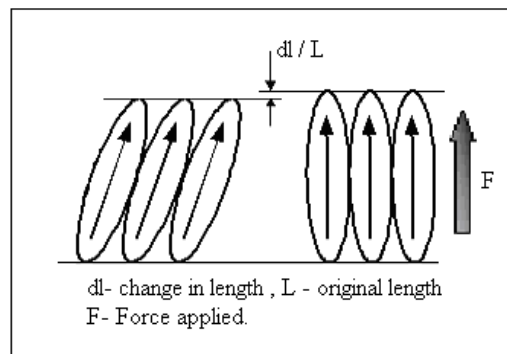


Figure 1.6 Magnetostrictive materials showing change in length. (Zhou and Lau, 2001)

### Electrostrictive materials

Electrostriction is a property of dielectric materials in which they form an elastic deformation when placed in an electric field. Non-piezoelectric materials, particularly barium titanate, can be used as electrostrictive materials. The electrostrictive response is highly dependent on the level of applied stress and output strain (Cohen, 2001), with large strain behaviour being the result of a  $90^\circ$  domain switching, leading to a macroscopic polarization, and change in macroscopic strain. The degree of strain depends on the grain orientation (Steuwer et al, 2006). Thus domain switching can form the basis of large strain actuation in a crystal as shown in figure 1.7.

The disadvantages of electrostrictive materials are that they are slow in response and have a low electromechanical efficiency (Cohen, 2001). Also thermal expansion due to resistive losses can cause very high disturbances to outputs in various applications.

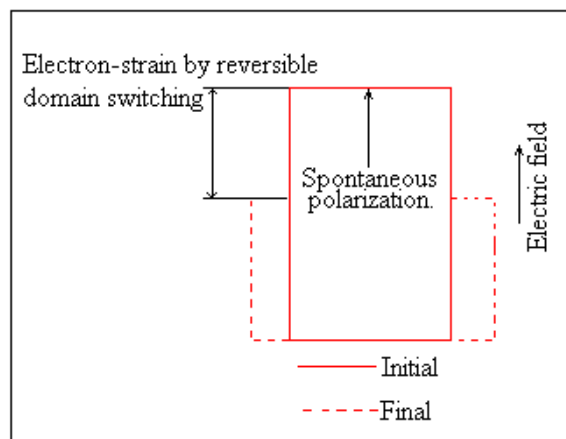


Figure 1.7 Domain switching for electrostrictive polymers. (Adapted Steuwer et al, 2006)

### Shape memory alloys

Shape memory alloys are materials which have the ability to change to a predetermined shape when heated and return to their original shape when cooled. The phase change can be achieved by electric heating. When the material is heated it undergoes a change in crystal structure which causes the change in the length of the material.

The shape memory material most commonly used is an alloy of nickel and titanium materials, known as Nitinol. These materials as described by Gilbertson et al (2003) have very good electrical and mechanical properties, long fatigue life, and high corrosion resistance. The small size of the wires similar to muscle fibres also appear attractive for use as artificial muscles.

The other types of artificial muscles include mechanical mechanisms, including rack and pinion gears, levers, pneumatic muscles and hydraulic muscles. However, these are likely to be large in size but would be mechanically efficient.

Among the alternatives discussed above the shape memory alloy was suggested as artificial muscle due to their sizes and constrain in space available for muscle attachment. Also the shape memory wires are like single fibres similar to that of actual muscles, thus are an ideal choice for shape memory wires was made as artificial muscles. The artificial muscle options that could be controlled electronically are compared in Table 1, with some of their key properties.

Property	Magnetostrictive materials	Electrostatic material	Shape memory alloys
Maximum strain (%)	0.24	5	8
Maximum stress (MPa)	28	43	200
Work density(KJ .m <sup>-3</sup> )	9210	2000	6450
Maximum efficiency (%)	2	--	5
Life cycle	10 <sup>7</sup>	--10 <sup>7</sup>	
Elastic modulus (MPa)	25	400	5150

**Table 1 Comparison of artificial muscles. (Steuer et al, 2006; Zhou and Lau, 2001; Gilbertson, 2003)**

Work density is the amount of work generated in one actuator cycle per unit volume of actuator. Efficiency is the ratio of work generated to input work supplied. Life cycle is the number of cycles or strokes the materials can endure. Thus, a shape memory alloy appears the best option for muscle due to its the high life cycle, comparable modulus of elasticity and enhanced efficiency of performance.

#### IV. SMA MUSCLES

The shape memory alloy (SMA) popularly known as Flexinol or Nitinol is an alloy of nickel and titanium, developed by Naval Ordinance Laboratory. When a current is passed through a shape memory wire heating it to its activation temperature, the wire changes shape to that which it has been trained to remember i.e. the linear contractions and expansions. Thus it could be used to mechanically mimic actual muscles as linear elements. Gilbertson et al. (2003) comment that the wire simply reduces in length, conserving its volume and getting thicker by 4 to 8 %. Shape memory alloys, when cooled from the high temperature austenite form, undergo a phase transformation in which their crystal structure becomes weaker and transforms into its low temperature martensite form as shown in figure 1.8.

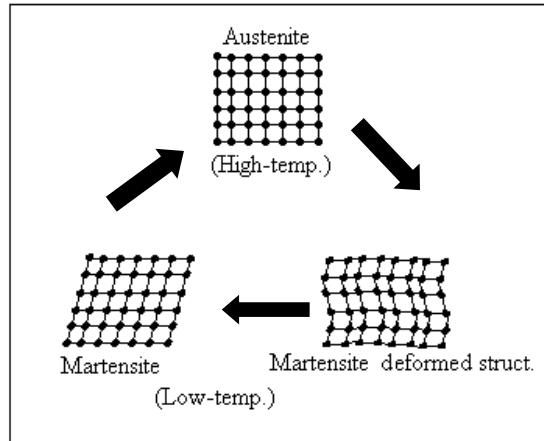


**Figure: 1.8 Mechanics of the shape memory effect. (Gilbertson, 2003)**

The phase transformation occurs over a narrow range of temperature, although the start and finish of the transformation actually spreads over a much larger range as experimentally demonstrated in Chapter 4 and the hysteresis occurs because the temperature curves for heating and cooling do not overlap. However, for Nitinol wires of very small diameter ranging from 25  $\mu\text{m}$  to 375  $\mu\text{m}$ , the hysteresis is almost negligible as cooling below the martensite temperature is almost instantaneous. Therefore, contraction and relaxation of the wire depends solely upon the temperature of the Nitinol wire.

The unique properties of shape memory wires include pseudo-elastic behaviour and a shape memory effect that can be used in many different fields of science and engineering. Biocompatibility of these alloys also makes them suitable for application to medical problems, as discussed by Machado et al (2003), as orthopaedic implants, cardiovascular devices, surgical instruments as well as orthodontic devices.

In the martensite phase there is an absence of stress, and it is stable at low (i.e. room) temperature. For the austenite phase, higher stresses are caused due to the increased temperature. Initially the shape memory wire should be subjected to tensile loading in order to provide some fraction of pre-strain, to a certain percentage of its original length to gain its initial position, as discussed by Shu et al. (1997).

A study conducted by Nae et al (2004) states that when the applied stress is relieved from a shape memory alloy the material returns to the austenite phase that then assumes the crystalline cubic shape. As shown in figure 1.9, the decrease in temperature increases the length of the wire. This phenomenon is called pseudo-elasticity or super-elasticity. Deforming pseudo-elastic material results in the formation of a martensite crystal. The pseudo-elastic behaviour of the shape memory alloy can also generate a large amount of non-resilient deformation and so that it can recover its original shape at the end of the loading process.

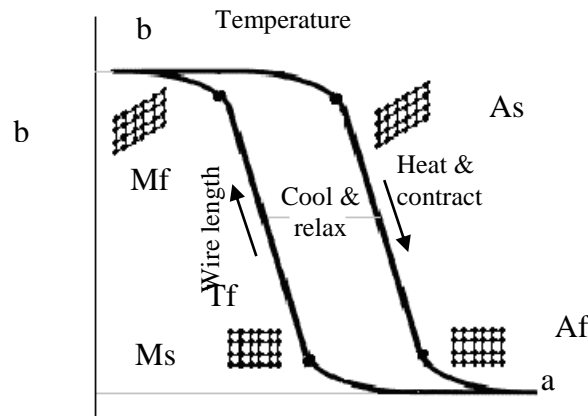


**Figure 1.9 Wire lengths vs. Temperature. (Adapted from Gilbertson, 2003)**

Mf – Martensite finish temperature (wire fully relaxed), Ms – Martensite start temperature (wire begins to relax), As – Austenite start temperature (wire begins to contract), Af – Austenite finish temperature (wire fully contract), a – Martensite form, b-Austenite form.

According to a study by Ma et al (2003) the inherent property of the material occurs as a result of the crystalline

phase transformation as shown in figure 1.9 which occurs between the low temperature martensite and high temperature austenite phases. Thus when the wire is heated above the austenite start temperature by passing an electrical current through it, the SMA attempts to contract to its original length, thereby applying an actuation force. The force exerted by each wire depends on its composition and size. Larger diameter wires with larger lengths will exert more force than smaller ones having the same composition. The trained force applied to reset the wire to its original length is directly proportional to the biasing force applied by the elastic elements of the wire. The activation and relaxation temperature for Nitinol alloys can fall in a range between -200 to 110 °C depending on the formulations of the alloy, with differences of less than 1% in ratio of the component metals in the alloy, greatly affecting the actual transition temperature (Ma et al, 2003).

The Dynalloy technical report (2004) show that the shape memory response can be improved by optimising the cooling of the wire - by using the natural environment, forced air, heat sinks, liquid coolants and Peltier elements. In the model developed by Shu et al (1997) the temperature of the wire was increased by either a surrounding hot water bath or by resistive heating with an electrical current. In both the cases the temperature of the shape memory alloy was the driving factor, showing that the method of heat transfer needs improvisation. The optimization of the characteristics of shape memory wire discussed by Gorbet and Russell (1995) depended on two factors, i.e. limits on the heating current, to protect the wire, and relaxation speed which is the cooling of the wire. The stress strain curves during austenite phase and martensite phase are shown in figure 1.10.

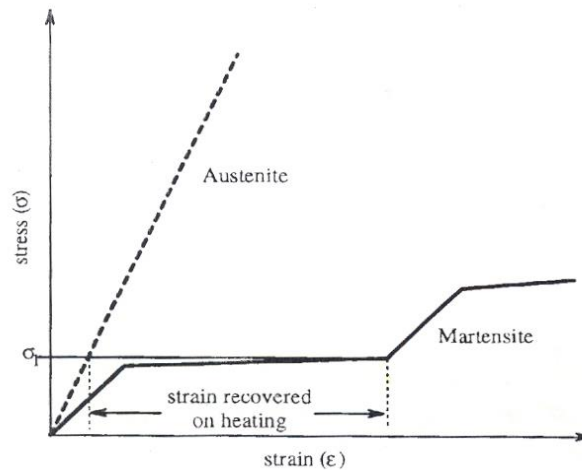


**Figure 1.10 Temperature phase for austenite and martensite curves. (Gorbet and Rusell, 1994)**

In the control mechanism studied by Holman and White (1993) the amount of heat generated was proportional to the volume of the wire, while the heat dissipated was proportional to the surface of the body exposed to the atmosphere. The property to dissipate heat was used to increase the cooling effect of the shape memory alloy actuator response, by using mechanical heat sink as heat exchangers, as shown in the figure 1.11. The heat sink shown in figure 1.11 can alter positions depending on the movement of the mobile link connected to the washer. The sink absorbs heat from the wire and due to larger surface area the convection is maximum. The movement of the mobile link shown in figure 1.11 helps the contact of the heat sink with the heated wire to absorb heat.

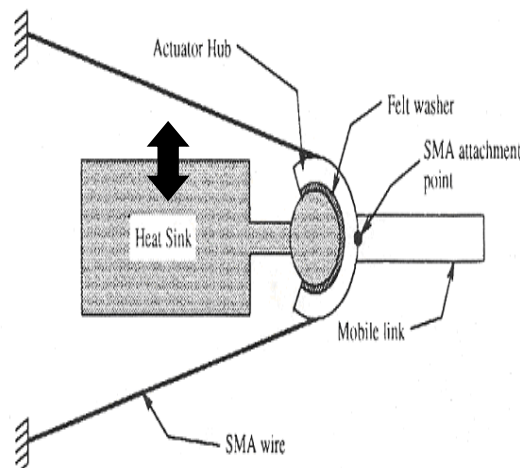


**Figure 1.11 Mechanical heat sink (Gorbet and Russell, 1994)**

The other techniques for cooling SMA wires can be achieved most effectively by using a Peltier element. In this system dissimilar metals held at different temperatures, develop a micro-voltage at the material junction in a phenomenon called the ‘Seebeck effect’. Alternatively, when a voltage is applied a temperature difference between the junctions is seen. Thus the inverse of the ‘Seebeck effect’ results in a heat pump called a Peltier element. The main advantages of using a Peltier element is its compactness, as it is a solid state heat extraction device with no liquids, and is free from refrigerants such as chlorofluorocarbons. The only disadvantage of using Peltier elements is that the hot surface should be in complete contact with the peltier element for it to extract heat. Bhattacharyya et al (1995) and Lagoudas and Bhattacharyya (1998) commented that the Peltier element cannot be used for applications where the wires have a very small area. Nae et al (2004) used forced convection for the heat transfer from shape memory wires, which is also an effective technique for reducing the temperature. Figure 1.12 compares the natural free convection (coefficient  $h_n=1.5 \text{ W/m}^2\text{K}$ ) and forced convection (coefficient,  $h_f = 150 \text{ W/m}^2 \text{ K}$ ) when experimentally measured for a  $100 \mu\text{m}$  shape memory wire. Hyo and Lee (2003) discussed that the speed of response for using a computer-programmed fan with a K type thermocouple can increase shape memory alloy wrapped around the wire.

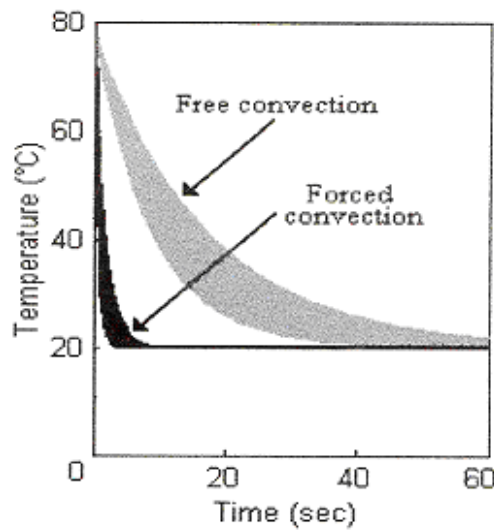


**Figure 1.12 Comparison for responses of free and forced convection. (Velazquez and Pissaloux, 2005).**

Kuribayshi (1991) proved that the maximum stable frequency response of an actuator was achieved when the wire was placed in a forced air environment and a very high current was passed into the wire to heat the wire quickly and then switched off.

Power produced by a shape memory alloy model can be calculated by using the second law of thermodynamics and Carnot cycle. The integral gives work-done to cause displacement from one position to another.

$$\Delta W = \int Pdv = \rho CV \frac{dT}{dt} = W_s - |W_q|$$

.....(1)

The above equation (1) is the amount of energy transferred from one system to another in which:  $W$  is the work done,  $\rho$  is the density of SMA,  $C$  is the specific heat capacity,  $V$  is the volume of SMA wire,  $W_s$  is the work supplied to the shape memory wire,  $W_q$  work processed by heat transfer. This is calculated from;

$$W_q = Q_{cd} + Q_{cv} + Q_{rd}$$

where  $Q_{cd}$  is the heat transfer due to conduction which can be neglected (Velazquez and Pissaloux, 2005), because shape memory wire has low internal resistance and experiences a uniform temperature distribution;  $Q_{rd}$  is the heat transfer due to radiation which can be neglected (as only one set of wire is actuated with a time interval and also the shape memory wire has a constant current passing through it for heating);  $Q_{cv}$  is the heat transfer due to convection. This last term can be calculated by considering a cylindrical model of the wire with a given length, exposed to the atmosphere. This can be expressed as;

$$Q_{cv} = qw = hc(t_w - t_b)$$

where,  $t_w$  is the wire temperature.

$t_b$  is the bulk temperature.

$$hc = \frac{k}{d} \times Nu.$$

where,  $hc$  is the heat transfer coefficient which can be given by  $W/m^2K$ ,  $k$  is the thermal conductivity of material and  $d$  is the diameter of the wire studied under convection.

The non-dimensional ( $Nu$ ) Nusselt number for laminar flow is a function of the boundary conditions which can be expressed in terms of the Prandtl and Reynolds numbers (Rohsenow and Hartnett, 1973). The above calculations can be used for the calculation of the force produced by a single wire or a bundle of wires. This is used in Appendix C for calculating the force and heat transfer coefficient.

## V. EXPERIMENTAL MODEL

The shape memory alloy used for the artificial muscles exhibits a complex behaviour, which depends on its the geometry, its pre-tension, applied temperature and the applied cooling. To determine the properties of the Nitinol SMA used in this work a test rig was constructed to measure the amount of force exerted by different length and sizes of wire. Firstly a clamp was designed to hold wire of size  $50\mu m$  up to  $375\mu m$  in diameter. This was then used in the experimental set-up shown in figure 1.13, where a spring balance measured the force generated in the wire. Power was applied to the wire by two 1.5V D-type batteries. The force produced by these different diameter wires of different lengths is shown in figure 1.13. The lengths are increased by increasing strands i.e. 1 strand = 100 mm length of wire.

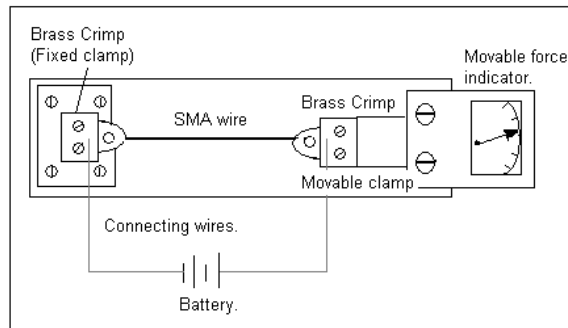


Figure 1.13 Experimental setup for shape memory alloy.

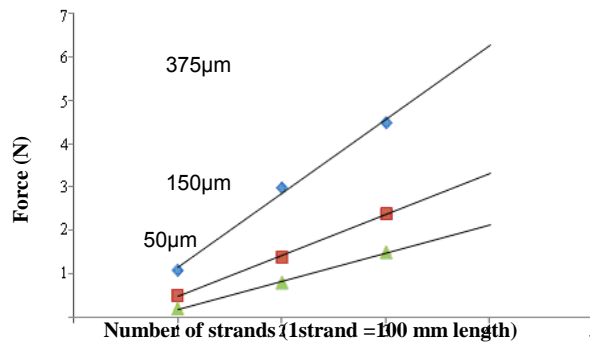
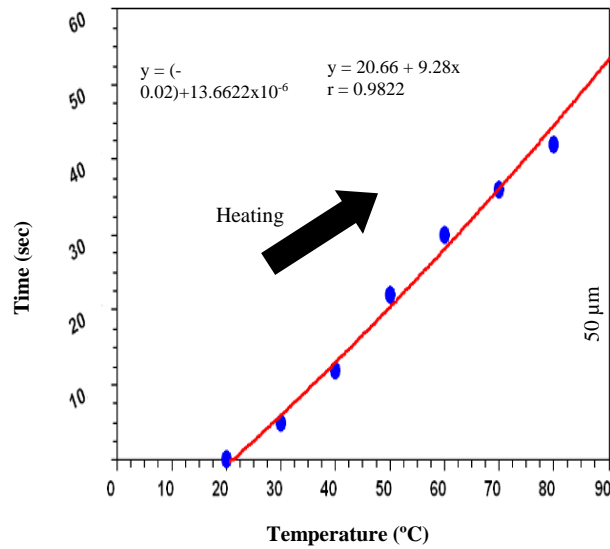


Figure 1.14 Basic properties of different diameter SMA wires

Figure 1.14 shows best-fit curves, which indicate that as the diameter and length of the wire increases, so the force produced increased as expected.

An experimental set-up with a load attached at one end of the SMA wire and a J-type thermocouple was used to measure the temperature and the cooling for the wire. This was carried out at room temperature with natural convection. The experiment used  $375\mu m$  wire with a constant current of 2.0 A. The time required to heat the wires was measured with a stopwatch.



**Figure 1.15 Experimental analysis for time of heating SMA wire**

For testing the properties of the SMA a wire of 375  $\mu\text{m}$  and length 15.25 mm with temperature increasing at 5°C per minute was observed for all experiments. The heating (20 to 90°C) and cooling (90 to 20°C) was observed at room temperature with natural convection. The data sheet provided by the manufacturer Dynalloy (2004), indicates the activation temperature should be between 55 to 90°C.

The displacement analysis produced the temperature / contraction behaviour. Figure 1.16 shows a temperature displacement curve, the slope of this curve is used for calculating the temperature expansion coefficient. Considering figure 1.16 between 55 and 90°C the slope is  $13.662 \times 10^{-6} \text{ m/}^\circ\text{C}$ . The heating was constant and the cooling observed was at room temperature with natural convection.

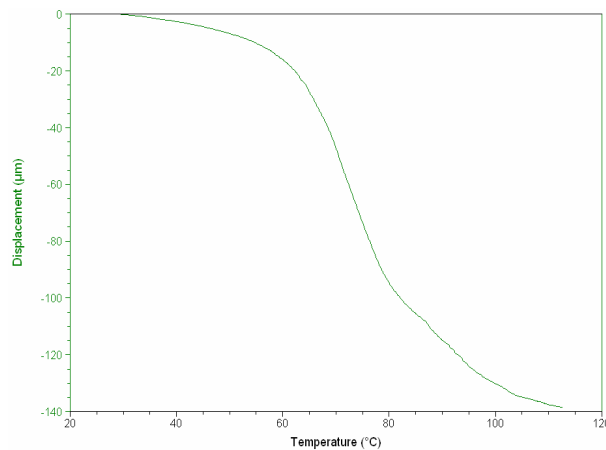


**Figure 1.16 DMA analysis of SMA wire, showing the thermal contraction of the wire.**

The DMA analysis in figure 1.17 shows cyclic heating and cooling (with cooling by natural convection) after a period of 1.5 minutes delay. The test was carried out for a 375  $\mu\text{m}$  diameter wire of length 15.25 mm with a temperature increasing at 5°C per minute. Thus the entire repetitive analysis for test number 1 to 5 between activation temperatures 20 to 90°C shows that the SMA has a repeatable behaviour with < 20  $\mu\text{m}$  displacement difference.

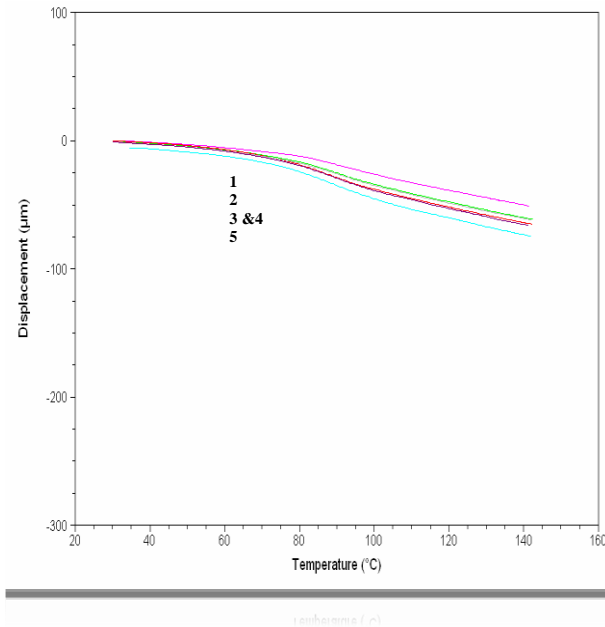


**Figure 1.17 DMA test for repeatability in temperature and displacement curves.**

The results of the DSC test are shown in figure 1.18, and present the variation in heat capacity with temperature. For this study a sample of wire diameter 375 µm and weight of 38 mg was placed in the DSC and heated from 22°C (room temperature) to 140°C (i.e. the temperature before overheating of wire). This shows that the phase change occurs between 55°C to 90°C, starting at 55°C and reaches it's maximum at 60°C, at which time the heat flow is maximum.

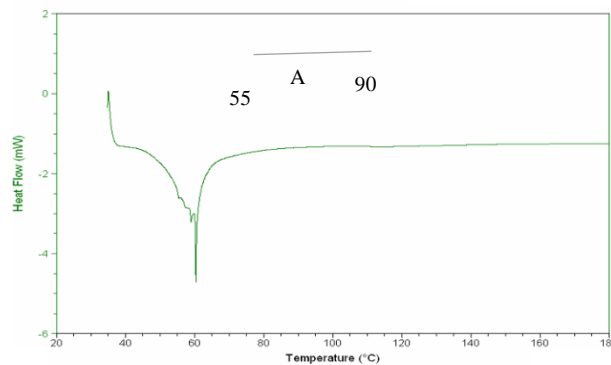


**Figure 1.18 DSC analysis for Shape Memory alloy wire.**

When heated the shape memory alloy has an extremely high power to weight ratio as discussed in Section 3.5 and with a suitable preload and retracting force it can regain its original position. The attachment points of the muscle wires on the ABS vertebral bodies used a turnbuckle arrangement, where the screws were hollow, allowing the wires to pass through them and attach to an electrical connector at the head of each. Unscrewing the screw allowed the wires to be tensioned (this is equivalent to the ‘tone’ of the natural muscle).

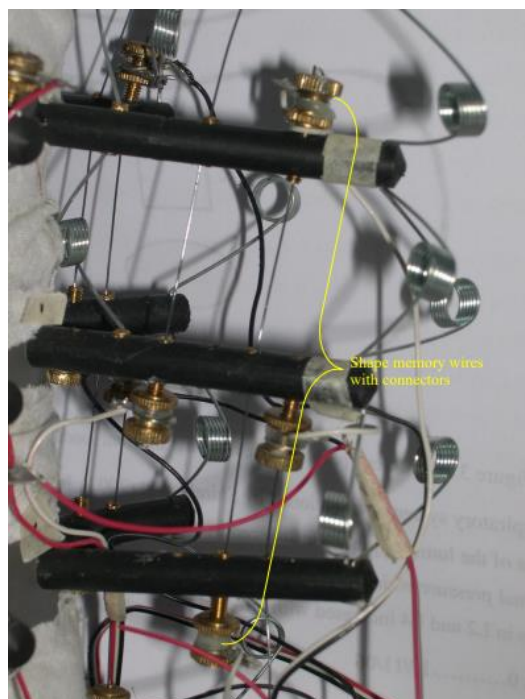


**Figure 1.19 SMA wires used as artificial muscles.**

The wires were then attached between the spinous and transverse processes as shown in figure 1.19 passing through brass bushes in the intermediate processes (to protect the ABS plastic) and connected with springs.

## CONCLUSION

In conclusion the shape memory alloys were used as artificial muscles and a laboratory spine with simplified geometry was developed. The spinal muscle architecture, as described above has a very complex arrangement that was simplified with each wire used as a muscle strand for modelling and was analysed with its characteristics and experimental validation.

The complex arrangement of muscles was developed to physiologically mimic the movements of the actual spine. The artificial muscles architecture was divided into several functional fascicles in order to mechanically and physiologically mimic the lower back muscle.

## REFERENCES

1. **Bhattacharyya A. Lagoudas DC. Wang Y. Kinra VK. 1995.** On the role of thermoelectric heat transfer in the design of SMA actuators, theoretical modelling and experiment. *Smart Materials and Structure*, 4, 252-263.
2. **Bogduk N. and Twomey LT. 1997.** *Clinical anatomy of the lumbar spine and sacrum*, (3<sup>rd</sup> Edition), Churchill Livingstone publication. ISBN 0-443-06014-2
3. **Cohen YB. 2001.** Transition of EAP material from novelty to practical applications- are we there yet? EAPAD, SPIE's 8<sup>th</sup> Annual International Symposium on Smart Structures and Materials. 4329-4402.
4. **Dean C. and Pegington J. 2002.** *Core Anatomy Vol:1- The limbs and vertebral column*. W B Saunders Publication. ISBN 0-7020-2040-0.
5. **Dynalloy Technical report. 2004.** Technical characteristic report of Flexinol actuator wires, Dynalloy Inc. of Dynamic Alloys.
6. **Gilbertson RG. Miranda C. Tuchman M. 2003.** *Muscle wire project book*, Mondo-tronics Publication. ISBN 1-879896-14-1.
7. **Gorbet RB. and Russell AR. 1995.** A novel differential shape memory alloy for position control. *Robotica*, 13, 423-430.
8. **Gray H. Pick TP. 1987.** *Gray's anatomy*, (15<sup>th</sup> edition) Chancellor Press, London.
9. **Heremans J. 1983.** A capacitive instrument for the measurement of magnetostriction in pulsed control. (Retrieved on 28 March 2005) *Journal of Physics for Engineers: Scientific Instruments*. 16. [www.npl.co.uk/materials/functional/magneto/magneto\\_index.html](http://www.npl.co.uk/materials/functional/magneto/magneto_index.html).
10. **Holman JP. White PRS. 1993.** *Heat transfer*. McGraw Hill publications. ISBN 0-07-112644-9.

11. **Hyo JL. and Lee JJ.2003.** Time delay of a Shape memory alloy actuator. International Journal of Robotic Results, 10:1, 13 - 20. ISBN 0-517-22365-1
12. **Kuribayashi K. 1991.** Improvement of the response of an SMA actuator using a temperature sensor. International. Journal of Robotic Results, 10,4, 18 - 24.
13. **Lagoudas DC. and Bhattacharyya A.1998.** A modelling of thin layer extensional thermoelectric SMA actuators. International Journal Solid Structure, 35, 331-362.
14. **Ma N. and Song G. 2003.** Control of shape memory alloy actuator using pulse width modulation. Smart Material and Structure, 12, 712 – 719.
15. **Machado LG. Savi MA.2003.** Medical applications of shape memory alloy. Brazilian Journal of Medical and Biological Research, 36, 683-691.
16. **Molly MM. Blume. 2001.**(Retrieved: 25 Jan. 2004) Oh my aching back! Vertebral disc and the effect of aging. EN 175. <http://www.engin.brown.edu/courses/en175/project%2001/miller.htm>
17. **Nae M. Song G. Lee HJ. 2004.** Position control of shape memory alloy actuator with internal electrical resistance feedback using neural network. Smart Material and Structure, 13, 777-783.
18. **Noordeen H. Elsebaie H. Crockard A. Winter R. Lonstein J. and Crisco J. 1997.** Primal Pictures Ltd. London.
19. **Noordeen H. Elsebaie H. Crockard A. Winter R. Lonstein J. Taylor B. Soames R. Renton P. Tucker S. and Crisco J. 2001** Interactive spine: Primal Pictures Ltd. London, ISBN 1-902470-32-X
20. **Rohsenow WM. and Hartnett JP. 1973.** Handbook of heat transfer, 7-20. ISBN 0-07-053576-0.
21. **Schmorl G. and Junghanns H. 1971.** The human spine in health and diseases. 2<sup>nd</sup> American Education for Grune& Stratton, New York, 18-20.
22. **Shirazi-Adl, Sadouk S, El-Rich M, Pop DG, Parnianpour M. 2002.** Muscle forces evaluation and the role of posture in human lumbar spine under compression. European Spine Journal, 11, 519-526.
23. **Shu SG. Lagoudas DC. Hughes D. and Wen JT. 1997.** Modelling of a flexible beam actuated by shape memory alloy wires. Smart Material and Structure, 6, 265-277.
24. **Steuer A. Hall DA. Withers PJ. Mori T. 2006.** Analysis of domain switching and elastic lattice strain in ferroelectric ceramics. SRMS -5 Conference, Chicago July 30 to August 2, 2002.
25. **Van CM. and Hayes CW. 1997.** Basic Orthopaedic Biomechanics. Lippincott Raven Publication, ISBN 0-397-51684-3.
26. **Velazquez R. Pissaloux E. 2005.** (Retrieved: 11<sup>th</sup> Nov. 2005) Design of shape memory alloy helical springs using force and time response criteria. <http://www.jussieu.fr/publications>
27. **Wayman CM. RW Cahn. P Haasen. 1983.** Phase transformation, no diffusive physical metallurgy. New York: North Holland, 1031-1075.
28. **Zhou LM. and Lau KT. 2001.** Investigation of strengthening and strain sensing techniques for concrete magnetostrictive structure using FRP composites and FBG sensors. Material and structure. 34, 42-50.